

# Effective field theory for few-boson systems

Betzalel Bazak,<sup>1,\*</sup> Moti Eliyahu,<sup>2</sup> and Ubirajara van Kolck<sup>1,3,†</sup>

<sup>1</sup>*Institut de Physique Nucléaire, CNRS-IN2P3, Univ. Paris-Sud, Université Paris-Saclay, 91406 Orsay, France*

<sup>2</sup>*The Racah Institute of Physics, The Hebrew University, Jerusalem 9190401, Israel*

<sup>3</sup>*Department of Physics, University of Arizona, Tucson, AZ 85721, USA*

(Dated: November 7, 2018)

We study universal bosonic few-body systems within the framework of effective field theory at leading order (LO). We calculate binding energies of systems of up to six particles and the atom-dimer scattering length. Convergence to the limit of zero-range two- and three-body interactions is shown, indicating that no additional few-body interactions need to be introduced at LO. Generalizations of the Tjon line are constructed, showing correlations between few-body binding energies and the binding energy of the trimer, for a given dimer energy. As a specific example, we implement our theory for  ${}^4\text{He}$  atomic systems and show that the results are in surprisingly good agreement with those of sophisticated  ${}^4\text{He}$ - ${}^4\text{He}$  potentials. Potential implications for the convergence of the EFT expansion are discussed.

## I. INTRODUCTION

Universal systems are not sensitive to the details of their microscopic physics. To a desired accuracy, their properties are frequently governed by a much more restricted set of parameters than the “underlying” theory of the microscopic dynamics. Effective field theory (EFT) is the framework to formulate universal systems in a systematic expansion in a ratio of small parameters so that at lowest orders only a few parameters appear. In this paper we discuss the properties of universal few-boson systems from the perspective of EFT.

Consider particles interacting through an interaction with range  $R$ . The effective range expansion (ERE) describes the two-body scattering process at relative wavenumber  $k \ll 1/R$  through a power series in  $k^2$ ,

$$k \cot \delta(k) = -\frac{1}{a_2} + \frac{r_2}{2}k^2 + \mathcal{O}(k^4), \quad (1)$$

where  $\delta(k)$  is the  $s$ -wave phase shift,  $a_2$  is the scattering length,  $r_2$  is the effective range, and further parameters appear in the higher-power terms. Typically, all ERE parameters have a size set by  $R$ , for example  $|a_2| \approx |r_2| \approx R$ . A type of universality occurs when the system is fine-tuned such that the scattering length is large compared to the other ERE parameters,  $|a_2| \gg |r_2| \approx R$ . In this case the two-body system of reduced mass  $\mu$  has a shallow real or virtual bound state at a binding energy  $B_2 \approx \hbar^2/(2\mu a_2^2) \ll \hbar^2/(2\mu R^2)$ , with corrections on the order of  $R/|a_2|$ . As first shown by Efimov [1], a number of shallow bound states appear when more particles are present. The properties of these systems are characterized by only a few parameters; for a review, see Ref. [2].

It is indeed common in physics to have an underlying theory, valid at a momentum scale  $M_{hi}$ , while we are

interested in processes occurring at typical momenta  $Q$  which are comparable to a much lower momentum scale  $M_{lo}$ ,  $Q \approx M_{lo} \ll M_{hi}$ . For example, nuclear structure involves momenta that are much smaller than the typical momentum scale of QCD,  $M_{QCD} \approx 1 \text{ GeV}/c$ . In this case, the range of the two-nucleon force  $R \approx \hbar/m_\pi c \simeq 1.4 \text{ fm}$ , which is set by the pion mass  $m_\pi$ , is thought to be relevant for heavy nuclei. However, the two-nucleon scattering lengths in both spin-singlet and spin-triplet  $s$  waves, respectively  $a_{2s} \simeq -23.4 \text{ fm}$  and  $a_{2t} \simeq 5.42 \text{ fm}$ , are larger in magnitude than  $R$ . Nuclear few-body systems thus fall into the same universality class as other systems characterized by large scattering lengths.

Another system in this class, which has even larger scale separation, is the  ${}^4\text{He}$  atomic system [3]. Here  $a_2 \approx 180 a_0$ , where  $a_0$  is the Bohr radius, is much larger than the van der Waals radius,  $R \approx 10 a_0$ . In addition, over the last two decades much attention has been devoted to an artificial system where these scales can be tuned by hand, namely ultracold atoms near a Feshbach resonance. Here  $a_2$  can be tuned to any value by changing an external magnetic or electric field [4].

Effective field theory allows us to focus on the low-momentum region in the more general case where there exist light particles (such as pions in nuclear physics) that generate long-range forces, which invalidate a straightforward ERE at two-body level. In EFT one starts by constructing the most general effective Lagrangian by integrating out the high-energy degrees of freedom, while keeping the symmetries of the underlying theory. The details of the underlying dynamics are contained in the interaction strengths, called low-energy constants (LECs). Through an estimate of the effects of interactions on observables, called power counting, a controlled approximation for the system at hand is obtained. Even when we are at such low energies that the ERE applies, the EFT with  $M_{hi} \sim \hbar/R$  allows us to account for deviations from the zero-range limit in a systematic expansion in  $M_{lo}/M_{hi} \sim R/|a_2|$ , not only for the two-body system but also for more-particle bound states, as long as they are sufficiently shallow, and for reactions involving these

\* bazak@ipno.in2p3.fr

† vankolck@ipno.in2p3.fr

states.

The EFT that reproduces the ERE for any short-range force was formulated at the two-body level in Ref. [5]. It was shown that at leading order (LO) a single two-body delta-function interaction appears which captures the information about  $a_2$ , while at higher orders other ERE parameters enter through more-derivative contact forces. After renormalization, the two-body amplitude is equivalent not only to the ERE, but also to Fermi's pseudopotential and to an energy-dependent boundary condition at the origin. The extension to three-boson systems was formulated at LO in Refs. [6–8], where it was found that a three-body, no-derivative contact force with a parameter  $\Lambda_\star$  is needed for proper renormalization. The three-body force is on a limit cycle and  $\Lambda_\star$  controls the position of the tower of Efimov states, for example the binding energy  $B_3$  of the three-body ground state. As  $\Lambda_\star$  is varied at fixed  $a_2$ , correlations appear among three-boson observables, such as the bosonic analog of the Phillips line [9], which relates the atom-dimer scattering length  $a_3$  to  $B_3$ . The successful, fully perturbative extension to the next two orders of the expansion was carried out in Refs. [10] and [11], the latter explicitly demonstrating the appearance of a new three-body force, with a new parameter. The minimum orders at which three-body forces of various types appear have been determined in Ref. [12].

Two questions arise:

1. Are higher-body forces needed at LO to describe systems with more bodies? A first step in this direction was taken in Refs. [13, 14] where the four-boson system was shown to be properly renormalized, at least within the first cycle of the three-body force. As a consequence of the absence of a LO four-body force, correlations develop between four- and three-body observables such as the bosonic analog of the Tjon line [15], which relates the binding energy  $B_4$  of the four-body ground state to  $B_3$ . Although no higher-order calculation of this system exists, it is inevitable that at some order a four-body force will appear and introduce a new scale. The importance of this new scale has been the subject of debate [16, 17].
2. What is the regime of validity of the EFT as the number of particles increases? As shown in Ref. [14], a three-body Efimov state spawns two four-body states, one barely more bound and another much more bound than the three-body parent. Model calculations [18–21] indicate that the same phenomenon repeats as the number of bodies is increased further. Thus, one expects deeper and deeper states. A measure of the particle binding momentum for a system of  $N$  identical particles of mass  $m$  is

$$Q_N = \sqrt{\frac{2mB_N}{N}}. \quad (2)$$

The EFT expansion in  $R/|a_2|$  includes, for few-body systems, also an expansion in  $Q_N R$ , which increases as the binding energy per particle,  $B_N/N$ , increases.

In order to make progress in answering these questions, here we build the EFT for few-boson systems with a large two-body scattering length, and study such systems with up to six particles at LO. One calculation for  $N > 4$  particles exists in short-range EFT: the binding energy of  $N = 6$  nucleons at LO [22] is consistent with both the absence of LO higher-body forces and EFT convergence, but is not conclusive<sup>1</sup>.

We extend the LO results to up to six bosons by solving the Schrödinger equation with the stochastic variational method (SVM) [24]. With an eye to future extensions employing Monte Carlo methods, we use a local Gaussian regulator. Our approach is valid for any bosonic system with large scattering length, including those close to the unitary limit  $|a_2| \rightarrow \infty$ . In order to be concrete, we apply the EFT to  ${}^4\text{He}$  atoms, motivated by the recent experimental verification of the excited Efimov state in this system [25]. Helium systems have been studied extensively with various  ${}^4\text{He}$ - ${}^4\text{He}$  potentials, see for example Refs. [26–38]. In EFT, the three- ${}^4\text{He}$  system has been studied up to N<sup>2</sup>LO [6, 7, 11, 39] using a formulation based on a dimer auxiliary field and on a sharp-momentum regularization with two- and three-body parameters  $\Lambda_2 \gg \Lambda_3$ . The four- ${}^4\text{He}$  system was calculated at LO [13] by solving the Yakubovsky equations with a non-local Gaussian regulator.

For  $N \leq 4$  our results are consistent with previous works. For a suitable two-body interaction strength a shallow dimer exists with a spatial extent that is about 10 times larger than the range associated with the van der Waals interaction between its constituents. Two trimers are bound: one shallow, close to the dimer, and one much deeper, about 50 times more bound. The ground-state trimer, in turn, is followed by two tetramer states, one close to the trimer and one deeper. When the excited trimer binding energy  $B_3^*$  is used to fix the three-body force parameter, the ground-state trimer and tetramer binding energies converge in the zero-range limit. Both trimer and tetramer [26] ground-state energies are correlated with the excited trimer energy.

For  $N = 5, 6$  we find similar convergence of binding energies with increasing cutoff parameter, suggesting that no higher-body forces are needed in LO. As a consequence, we can construct generalized Tjon lines where the binding energies beyond  $N = 4$  are correlated with

<sup>1</sup> Note that finite-range potential models, such as those employed in the  $N > 4$  calculations of Refs. [18–21, 23], resemble an EFT with a finite regulator, and most of their results are likely to be compatible with EFT. However, in an EFT regulator insensitivity is needed for model independence, while physical range effects are subleading and should be treated in perturbation theory [5, 10].

$B_3$  at fixed two-body input. Such lines have been constructed before by combining results from different phenomenological two-body potentials [27, 28]; here, these lines arise from the continuous variation of the single LO three-body parameter  $\Lambda_*$ . Deeper states are smaller, and therefore finite-range corrections are expected to be more important for them. The ground-state energies grow to about 16 times the trimer energy at  $N = 6$ , but we will see that our results still agree with potential models within about 15%. Although we cannot offer a conclusive answer without higher-order calculations, our LO calculations are very encouraging for the convergence of the EFT in many-body systems. They also provide a baseline for future comparisons with higher-order results.

Our paper is organized as follows. In Sec. II we introduce the LO EFT, and its regularization and renormalization. We also discuss the two inputs needed to fix the two LO parameters. In Sec. III the numerical method for the solution of the Schrödinger equation is presented. Our results are given in Sec. IV, while Sec. V summarizes our findings and some of their implications.

## II. THEORY

A system of spinless bosons of mass  $m$  interacting via a short-range force can be described by the Lagrangian density

$$\mathcal{L} = \psi^\dagger \left( i\partial_0 + \frac{\nabla^2}{2m} \right) \psi - \frac{\tilde{C}^{(0)}}{2} (\psi^\dagger \psi)^2 - \frac{\tilde{D}^{(0)}}{6} (\psi^\dagger \psi)^3 + \dots \quad (3)$$

where  $\psi$  is the bosonic field operator,  $\tilde{C}^{(0)}$  and  $\tilde{D}^{(0)}$  are low-energy constants, and “...” stand for terms with more fields and/or more derivatives, which are subdominant. Since this work is focused on the leading order, these terms will be neglected in the following. For simplicity we use units where  $\hbar = c = 1$ .

The interactions in Eq. (3) are *delta* functions in coordinate space. For singular interactions, the solution of the Schrödinger equation requires regularization, that is, the introduction of a function that suppresses momenta above a cutoff  $\Lambda$ . This is achieved by smearing the delta function over distances  $\sim \Lambda^{-1}$ . Observables are independent of the arbitrary value of  $\Lambda$  (renormalization) if the LECs have specific dependences on  $\Lambda$ . In the following we use dimensionless LECs by writing

$$\tilde{C}^{(0)}(\Lambda) = \frac{4\pi}{m\Lambda} C^{(0)}(\Lambda), \quad \tilde{D}^{(0)}(\Lambda) = \frac{(4\pi)^2}{m\Lambda^4} D^{(0)}(\Lambda). \quad (4)$$

When the EFT is truncated at given order, observables acquire a residual cutoff dependence  $\mathcal{O}(Q/\Lambda)$ , which can be made arbitrarily small by increasing  $\Lambda$ . However, the truncation of the Lagrangian induces relative errors of  $\mathcal{O}(Q/M_{hi})$ . Thus, a variation of the cutoff from  $M_{hi}$  to much larger values gives an estimate of the theoretical error. (For values of  $\Lambda$  below  $M_{hi}$ , the error is dominated by the regularization error.) We discuss our specific regularization and renormalization procedures next.

### A. Two-body sector

At low energies, and since  $|a_2|$  is much larger than the range of the potential, physics cannot be sensitive to the short-distance details of the potential. Therefore the potential between the particles can be represented by a contact potential,  $V = \tilde{C}^{(0)} \delta(\mathbf{r})$ . To see the need for regularization, one can solve the momentum-space Schrödinger equation for the two-body bound state,

$$\frac{p^2}{m} \phi(p) + \tilde{C}^{(0)} \int \frac{d^3 p'}{(2\pi)^3} \phi(p') = -B_2 \phi(p) \quad (5)$$

where  $B_2$  is the dimer binding energy and  $\phi(p)$  is the momentum-space radial wave function. Solving for  $\phi(p)$ , the coupling constant  $\tilde{C}^{(0)}$  has to satisfy

$$\frac{1}{\tilde{C}^{(0)}} = - \int \frac{d^3 p'}{(2\pi)^3} \frac{1}{p'^2/m + B_2}. \quad (6)$$

However, since the integral on the right-hand side diverges, no solution exists for any finite  $\tilde{C}^{(0)}$ .

If we denote the incoming (outgoing) relative momenta in two-body scattering by  $\mathbf{p}$  ( $\mathbf{p}'$ ), one can regularize the integral by introducing cutoff functions  $f_\Lambda(\mathbf{p})f_\Lambda(\mathbf{p}')$ , where  $\Lambda$  is the cutoff parameter. Using a Gaussian function,  $f_\Lambda(x) = \exp(-x^2/\Lambda^2)$ , the equation for  $\tilde{C}^{(0)}$  is modified to

$$\frac{1}{\tilde{C}^{(0)}(\Lambda)} = - \int \frac{d^3 p'}{(2\pi)^3} \frac{\exp(-2p'^2/\Lambda^2)}{p'^2/m + B_2}, \quad (7)$$

which converges. The solution can be expanded in powers of  $Q_2/\Lambda$ , where  $Q_2$  is defined in Eq. (2):

$$\tilde{C}^{(0)}(\Lambda) = -\frac{4\pi}{m\Lambda} \sqrt{2\pi} \left[ 1 + \sqrt{2\pi} \frac{Q_2}{\Lambda} + \mathcal{O}\left(\frac{Q_2^2}{\Lambda^2}\right) \right]. \quad (8)$$

Therefore, to keep the dimer binding energy fixed, the coupling constant has to “run” with the cutoff parameter  $\Lambda$ . For another regulator the dependence of  $\tilde{C}^{(0)}$  on  $\Lambda$  will not, in general, be given by Eq. (8), but it will still be such as to reproduce  $B_2$ . Any physical observable has to be independent of  $\Lambda$  and of the regularization method used, within the error generated by the neglect of higher orders.

In coordinate space the contact potential is now smeared over a range  $\sim 1/\Lambda$ . For the non local Gaussian regulator the result is a non-local potential [8],

$$\langle \mathbf{r} | V | \mathbf{r}' \rangle = \tilde{C}^{(0)}(\Lambda) \delta_\Lambda(\mathbf{r}) \delta_\Lambda(\mathbf{r}'), \quad (9)$$

where

$$\delta_\Lambda(\mathbf{r}) \equiv \frac{\Lambda^3}{8\pi^{3/2}} \exp(-\Lambda^2 \mathbf{r}^2/4) \quad (10)$$

satisfies  $\lim_{\Lambda \rightarrow \infty} \delta_\Lambda(\mathbf{r}) = \delta(\mathbf{r})$ .

To get a local potential we use a regularization  $f_\Lambda(\mathbf{q})$  on the momentum transfer  $\mathbf{q} = \mathbf{p} - \mathbf{p}'$ , yielding instead

$$\langle \mathbf{r} | V | \mathbf{r}' \rangle = \tilde{C}^{(0)}(\Lambda) \delta_\Lambda(\mathbf{r}) \delta(\mathbf{r} - \mathbf{r}'). \quad (11)$$

Defining the dimensionless LEC according to Eq. (4) and summing over all pairs, the two-body interaction is

$$V_{2b} = \frac{4\pi}{m\Lambda} C^{(0)}(\Lambda) \sum_{i<j} \delta_{\Lambda}(\mathbf{r}_{ij}), \quad (12)$$

where  $\mathbf{r}_{ij}$  is the position of particle  $i$  with respect to particle  $j$ . We will employ the Gaussian regularization (10). To renormalize  $C^{(0)}(\Lambda)$  one has to choose an observable to be fixed to its physical value. The parameter  $C^{(0)}(\Lambda)$  is then, in fact, a function of the dimensionless ratio  $Q_2/\Lambda$ . However, for a local regulator the running of  $C^{(0)}(\Lambda)$  cannot be obtained analytically; we discuss it in Sec. IV A below.

### B. Three-body sector

Although the two-body system is suitably renormalized, the trimer ground-state binding energy  $B_3$  is found to be strongly dependent on the cutoff [6, 7],  $B_3 \propto \Lambda^2/m$ , a result first obtained by Thomas [40]. As  $\Lambda$  increases, other bound states appear in the spectrum. Since  $\Lambda$  is not a physical parameter, a three-body contact interaction has to be introduced at this order for renormalization [6, 7].

In Refs. [6, 7], the two-body amplitude in the large-cutoff limit was used as input to solve the three-body problem, and a sharp cutoff function  $f_{\Lambda}(x) = \theta(1 - x/\Lambda)$  was introduced in the resulting integral equation. The running of the three-body LEC was found to be

$$\tilde{D}^{(0)}(\Lambda) \propto \frac{(4\pi)^2 \sin(s_0 \ln(\Lambda/\Lambda_{\star}) - \arctan s_0^{-1})}{m\Lambda^4 \sin(s_0 \ln(\Lambda/\Lambda_{\star}) + \arctan s_0^{-1})}, \quad (13)$$

where  $s_0 \simeq 1.00624$  and  $\Lambda_{\star}$  is a parameter determined by one three-body datum. A similar structure was found with the non-local Gaussian regulator [8, 13]. This log-periodic structure has divergences, signaling the appearance of deep bound states.

Here we employ the same local Gaussian regulator as in the two-body system. With the dimensionless LEC introduced in Eq. (4) the three-body interaction can be written as a cyclic permutation of triplets,

$$V_{3b} = \frac{(4\pi)^2}{m\Lambda^4} D^{(0)}(\Lambda) \sum_{i<j<k} \sum_{cyc} \delta_{\Lambda}(\mathbf{r}_{ij}) \delta_{\Lambda}(\mathbf{r}_{jk}). \quad (14)$$

The parameter  $D^{(0)}(\Lambda)$  now depends not only on  $Q_2/\Lambda$  but also on  $\Lambda_{\star}/\Lambda$ . We discuss the solution of the three-boson system with our local regulator in Sec. IV B.

### C. ${}^4\text{He}$ atoms

The previous arguments and most of the issues we address below concern any universal bosonic system, and also apply to fermions with three or more states; for a

TABLE I. Length scales (in  $\text{\AA}$ ) for two  ${}^4\text{He}$  atoms, deduced from two modern  ${}^4\text{He}$ - ${}^4\text{He}$  potentials, LM2M2 and PCKLJS. The scattering length  $a_2$  and effective range  $r_2$  are from Refs. [30, 33, 36], while the van der Waals length  $r_{\text{vdW}}$  is evaluated from the value of the van der Waals coefficient  $C_6$  calculated in Refs. [42, 43].

	LM2M2	PCKLJS
$a_2$	100.23	90.42(92)
$r_2$	7.326	7.27
$r_{\text{vdW}}$	5.378	5.378

TABLE II. Binding energies (in mK) of  ${}^4\text{He}$  clusters.  $B_N^{(*)}$  denotes the binding energy of the  $N$ -body ground (lowest excited) state. The first two columns show results [37] for two modern  ${}^4\text{He}$ - ${}^4\text{He}$  potentials. The last column displays experimental results [25, 45, 46], as described in the text.

	LM2M2	PCKLJS	experiment
$B_2$	1.3094	1.6154	$1.3_{-0.19}^{+0.25}$ , 1.76(15)
$B_3^*$	2.2779	2.6502	
$B_3^* - B_2$	0.9685	1.0348	0.98(2)
$B_3$	126.50	131.84	
$B_4^*$	127.42	132.70	
$B_4$	559.22	573.90	

review, see Ref. [41]. (For fermions with less than three states, there is no LO three-body force.) To be definite, we focus on  ${}^4\text{He}$  atomic systems when presenting numerical results.

The  ${}^4\text{He}$  atomic system was the subject of much study, both theoretical and experimental. The length scales associated with the two-body system are the main ERE parameters,  $a_2$  and  $r_2$ , as well as the van der Waals length, defined as  $r_{\text{vdW}} = (mC_6)^{1/4}$ , where  $C_6$  characterizes the potential tail  $-C_6/r^6$ . In Table I we present these length scales for  ${}^4\text{He}$  atoms as obtained by two modern  ${}^4\text{He}$ - ${}^4\text{He}$  potentials, LM2M2 [29] and PCKLJS [36]. As expected in this universality class,  $a_2 \gg r_2 \sim r_{\text{vdW}}$ .

In Table II we summarize the energies of  ${}^4\text{He}$  clusters, as calculated from the same two potentials in Ref. [37]. We show in Table II also the results extracted from experimental data. The dimer binding energy  $B_2$  is calculated in Ref. [44] from the measurement of the average separation,  $\langle r \rangle = 52(4) \text{\AA}$  [45]. Very recently, a value of 1.76(15) mK was measured for the dimer energy [46]. The difference between excited-trimer and dimer energies,  $B_3^* - B_2$ , was also measured recently [25].

Renormalization at the two- and three-body levels requires the input of two observables to determine the running of  $C^{(0)}(\Lambda)$  and  $D^{(0)}(\Lambda)$ . We fit  $C^{(0)}$  to the dimer binding energy  $B_2$ , and  $D^{(0)}$  to the excited-trimer

binding energy  $B_3^*$ . The excited trimer is closer to the three-boson threshold than the ground trimer and thus, presumably, afflicted by smaller errors stemming from the EFT truncation. This induces a dependence of the three-body LEC  $D^{(0)}$  on the ratio  $Q_3^*/\Lambda$ , where  $Q_3^* = \sqrt{2mB_3^*/3}$  is the binding momentum of the trimer excited state, which is related to the  $\Lambda_*$  introduced in Sec. II B.

One would like to use the experimental data to calibrate the EFT. However, there are two problems. First, the experimental situation is not entirely clear, as can be seen from the discrepancy in the dimer binding energies in Table II. Second, there are no other experimental numbers to compare our predictions with, even if we neglect the spread in dimer binding energies. We use instead values calculated from the two modern potentials LM2M2 and PCKLJS, which give  $B_2$  and  $B_3^* - B_2$  in fair agreement with data and provide a reasonable representation of the data spread. For these potentials a number of other observables have been calculated, comparison with which offers an assessment of the success of the EFT at LO. Needless to say, as the experimental situation improves our calculations can be repeated with experimental input, short-circuiting the need for potential models.

From the values of  $B_2$  and  $B_3^*$ , the input binding momenta are  $Q_2 \simeq 0.0055 a_0^{-1}$  and  $Q_3^* \simeq 0.0059 a_0^{-1}$  for the LM2M2 potential, and  $Q_2 \simeq 0.0061 a_0^{-1}$  and  $Q_3^* \simeq 0.0064 a_0^{-1}$  for the PCKLJS potential. With this input, LO predictions can be made for systems with more particles. Our method of solution of the Schrödinger equation is described in the next section. Calculations are performed at various cutoff values. The residual cutoff dependence of an observable can be expanded in a power series in  $Q/\Lambda$ , where  $Q$  is the typical momentum associated to the physical process where that observable is measured. After fitting the coefficients of the power series to the numerical results at cutoff values  $\Lambda \gtrsim 1/R$ , we can extrapolate to  $\Lambda \rightarrow \infty$ , which corresponds to a zero-range potential.

However, in any physical situation the underlying interactions have a finite range  $R$ , effects of which are accounted for by higher-order EFT interactions. A rough estimate of the LO relative error is  $QR$ , where we take  $1/R \sim 2/r_2 \gg 1/a_2$  from Table I. An alternative error estimate is obtained from the residual cutoff dependence. If  $Q$  is identified correctly, the coefficients of the series in  $Q/\Lambda$  are expected to be of  $\mathcal{O}(1)$ . Then, by varying the cutoff from  $\sim 1/R$  to  $\infty$ , we obtain an estimate of the error, which should be comparable to the rougher  $QR$  estimate. Note that the two estimates can easily differ by a factor of  $\mathcal{O}(1)$ , which is the expected size of the series coefficients. Yet another way to gauge the size of higher-order effects is to use different inputs that are supposed to be the same at the order of interest, for example  $1/a_2$  or  $Q_2$  at LO. Better estimates can be obtained once a few subleading orders have been calculated, and one can be more confident about the magnitude of the product

$QR$  for a given observable.

### III. METHOD

To solve the  $N$ -body Schrödinger equation, we use  $N-1$  Jacobi vectors  $\boldsymbol{\eta}_n$ ,  $n = 1, \dots, N-1$ , which we collect in a “vector of vectors”  $\boldsymbol{\eta} = (\boldsymbol{\eta}_1, \boldsymbol{\eta}_2, \dots, \boldsymbol{\eta}_{N-1})^T$ . We expand the wavefunction on a correlated Gaussian basis,

$$\psi(\boldsymbol{\eta}) = \sum_i c_i \hat{\mathcal{S}} \exp\left(-\frac{1}{2} \boldsymbol{\eta}^T A_i \boldsymbol{\eta}\right), \quad (15)$$

where  $A_i$  is an  $(N-1) \times (N-1)$  real, symmetric, and positive-definite matrix and  $c_i$  is a coefficient to be determined. Here  $\hat{\mathcal{S}}$  is the symmetrization operator necessary to enforce bosonic symmetry.

One of the advantages of this basis is that the matrix elements of the Hamiltonian as well as the overlap of two basis functions can be calculated analytically in most cases. Denoting by  $|A\rangle$  a basis vector with matrix  $A$ , the overlap matrix element is

$$\langle A|A'\rangle = \left(\frac{(2\pi)^{N-1}}{\det B}\right)^{3/2}, \quad (16)$$

where  $B = A + A'$ . The matrix element of the internal kinetic energy is

$$\frac{\langle A|T_{int}|A'\rangle}{\langle A|A'\rangle} = 3 \text{Tr}G, \quad (17)$$

where  $G = AB^{-1}A'\Pi$ , with  $\Pi_{nl} = (2\mu_n)^{-1}\delta_{nl}$  an  $(N-1) \times (N-1)$  diagonal matrix and  $\mu_n$  the reduced mass corresponding to coordinate  $\boldsymbol{\eta}_n$ . The matrix elements of the potential involve the relative particle positions, which we write as  $\mathbf{r}_{ij} = \omega_{ij}^T \boldsymbol{\eta}$ . For a fixed pair  $ij$ ,  $\omega_{ij}$  is an  $N-1$ -component vector. The two-body interaction matrix element is then

$$\frac{\langle A|V_{2b}|A'\rangle}{\langle A|A'\rangle} = \frac{\Lambda^2 C^{(0)}(\Lambda)}{2\sqrt{\pi}m} \sum_{i<j} \left(1 + f_{ij} \frac{\Lambda^2}{2}\right)^{-3/2}, \quad (18)$$

where  $f_{ij} = \omega_{ij}^T B^{-1} \omega_{ij}$ . For the three-body interaction,

$$\begin{aligned} \frac{\langle A|V_{3b}|A'\rangle}{\langle A|A'\rangle} &= \frac{\Lambda^2 D^{(0)}(\Lambda)}{4\pi m} \\ &\times \sum_{i<j<k} \sum_{cyc} \left[ \det \left( I + F_{ijk} \frac{\Lambda^2}{2} \right) \right]^{-3/2} \end{aligned} \quad (19)$$

where  $I$  is the  $2 \times 2$  identity matrix and  $F_{ijk} = \Omega_{ijk}^T B^{-1} \Omega_{ijk}$  is a  $2 \times 2$  matrix, with  $\Omega_{ijk} = (\omega_{ik} \ \omega_{jk})$  a  $2 \times (N-1)$  matrix.

Another advantage of this basis is its flexibility: Since we want  $\Lambda^{-1} \lesssim R \ll a_2$  we need a large spread of basis functions, which can be achieved within this basis.

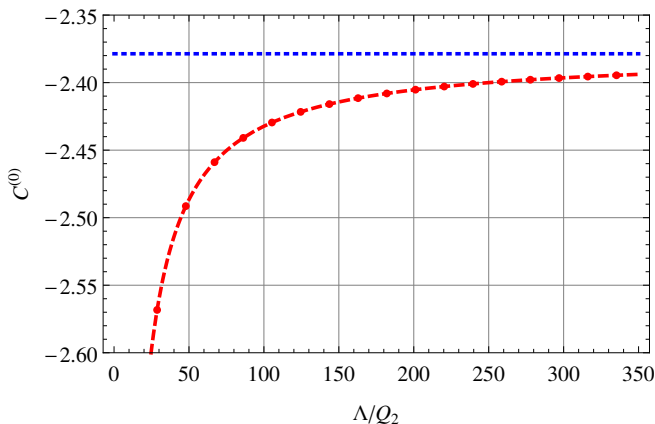


FIG. 1. (Color online) The dimensionless two-body low-energy constant  $C^{(0)}$  for various cutoff values  $\Lambda$ , in units of the dimer binding momentum  $Q_2$ . Shown are the results for  ${}^4\text{He}$  atoms (red circles) and a fit with Eq. (20) (red dashed line) which has the asymptotic value  $C_\infty^{(0)}$  (blue dotted, horizontal line).

To optimize our basis we use the stochastic variational method (SVM) [24]. To add a function to our basis, or to refine our basis by replacing an exist basis function with a new one, the elements of the matrix  $A_i$  are chosen randomly one by one, and the one which gives the lowest energy is taken. According to the variational principle, upper bounds for the ground and excited states are guaranteed.

#### IV. RESULTS

Here we present the results of the LO EFT (Sec. II) solved with the SVM (Sec. III) for  $N = 2 - 6$  particles.

##### A. Two bosons

We solve the two-body Schrödinger equation and demand that the dimer binding energy  $B_2$  be reproduced for any value of the cutoff. This determines the values of the LEC  $C^{(0)}(\Lambda)$ , which is shown in Fig. 1. The numerical results are well fitted by

$$C^{(0)}(\Lambda) = C_\infty^{(0)} \left[ 1 + \alpha \frac{Q_2}{\Lambda} + \beta \left( \frac{Q_2}{\Lambda} \right)^2 + \dots \right], \quad (20)$$

where  $C_\infty^{(0)} \simeq -2.379$ ,  $\alpha \simeq 2.241$  and  $\beta \simeq 1.456$ . This curve is universal in the sense that at the same cutoff  $\Lambda$  different input potentials, which differ in  $Q_2$ , correspond to points lying on this curve. The  $Q_2$ -independent asymptotic value  $C_\infty^{(0)}$  is also indicated in Fig. 1.

Equation (20) can be compared with Eq. (8), which was also obtained with a Gaussian regulator, but a separable one. In both cases, the expansion coefficients are

numbers of  $\mathcal{O}(1)$ , as expected from the fact that the two-body binding momentum  $Q_2$  provides the scale for cutoff variation of the LEC.

At this order, the two-body amplitude gives rise to the ERE expansion (1) with  $1/a_2 = Q_2$ . The other ERE parameters are cutoff dependent and vanish as  $\Lambda \rightarrow \infty$ . For example, the induced effective range is

$$r_2(\Lambda) = \frac{\gamma}{\Lambda} \left[ 1 + \mathcal{O} \left( \frac{Q_2}{\Lambda} \right) \right], \quad (21)$$

where  $\gamma \simeq 2.869$ . This is because the regularized two-body potential (12) has a range  $\sim \Lambda^{-1}$ . In the limit of  $\Lambda \rightarrow \infty$  we reproduce, therefore, the limit of a zero-range potential. The  $\Lambda^{-1}$  dependence in Eq. (21) implies two-body corrections to the zero-range limit appear at next-to-leading order (NLO). At this order a two-derivative delta-function potential must be introduced in first-order distorted-wave Born approximation, and its LEC adjusted to yield a finite effective range  $r_2$  [5]. At next-to-next-to-leading order (N<sup>2</sup>LO), corrections proportional to  $r_2^2$  determine the two-body amplitude [5].

##### B. Three bosons

In the three-boson system, we demand that the binding energy  $B_3^*$  of the trimer excited state be obtained at all values of the cutoff. This can be achieved in different ways, depending on which unrenormalized state we bring to the excited-state energy with the three-body force. Different unrenormalized states lead to different functions  $D^{(0)}(\Lambda)$ . The resulting three-body LEC is plotted in Fig. 2 for various values of  $\Lambda/Q_3^*$ , when the PCKLJS value of the binding energy of the trimer excited state is used as input. The two branches correspond to fitting the unrenormalized first and second excited states to the excited trimer. Similar cutoff dependence arises from the LM2M2 potential.

The structure shown in Fig. 2 is not the same as Eq. (13): Not only is the form different, but also our  $D^{(0)}(\Lambda)$  depends on the value of  $Q_2$ . In contrast to the regularization procedure that led to Eq. (13), here we can choose which unrenormalized state to use. Equation (13) comes from studies of a non-local potential, while we employ a local one with the same cutoff in the two- and three-body sectors, suggesting that this is the source of the differences. However, since  $D^{(0)}(\Lambda)$  is not an observable, it may depend on the regularization scheme; only observables need to be independent of the regularization scheme. In the following we use the upper branch of Fig. 2.

With the LECs fixed, we can predict the ground-state trimer energy. The ratio of the binding energies of the trimer ground and excited states is plotted in Fig. 3. The numerical results can be fitted by a series in powers

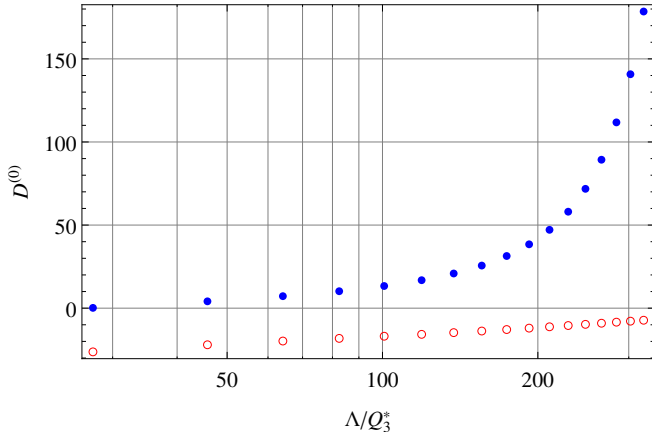


FIG. 2. (Color online) The dimensionless three-body low-energy constant  $D^{(0)}$  for various cutoff values  $\Lambda$ , in units of the binding momentum of the trimer excited state  $Q_3^*$ . The upper branch (solid blue circles) corresponds to fitting the first unrenormalized excited state to the  ${}^4\text{He}$  trimer excited state of the PCKLJS potential; the lower branch (open red circles) corresponds to fitting instead the second unrenormalized excited state.

TABLE III. Dimensionless parameters of the fit (22) to the trimer ground-state energy. The upper (lower) results correspond to the LM2M2- (PCKLJS-) based EFT.

$B_3(\infty)/B_3^*$	$\alpha_3$	$\beta_3$	$\gamma_3$
57.18	-0.26	—	—
57.10	-0.21	-0.39	—
57.16	-0.26	0.20	-2.04
51.51	-0.28	—	—
51.47	-0.25	-0.26	—
51.52	-0.31	0.45	-2.66

of the small parameter  $Q_3/\Lambda$ ,

$$\frac{B_3(\Lambda)}{B_3^*} = \frac{B_3(\infty)}{B_3^*} \left[ 1 + \alpha_3 \frac{Q_3}{\Lambda} + \beta_3 \left( \frac{Q_3}{\Lambda} \right)^2 + \gamma_3 \left( \frac{Q_3}{\Lambda} \right)^3 + \dots \right], \quad (22)$$

where  $Q_3$  itself is calculated from  $B_3(\infty)$ . To check the stability of such a fit, we cut this series after each term and fit to the calculated data. The resulting parameters are summarized in Table III. They have natural size and similar values for the two potentials. The corresponding curves, plotted in Fig. 3, are very close to each other for  $\Lambda/Q_3$  beyond about 8. This all suggests good convergence to the zero-range limit.

For the LM2M2 input, the asymptotic value of the binding energy is  $B_3(\infty)/B_3^* \simeq 57.15(4)$ , corresponding to  $Q_3 \simeq 0.045 a_0^{-1}$ , while for the PCKLJS input,

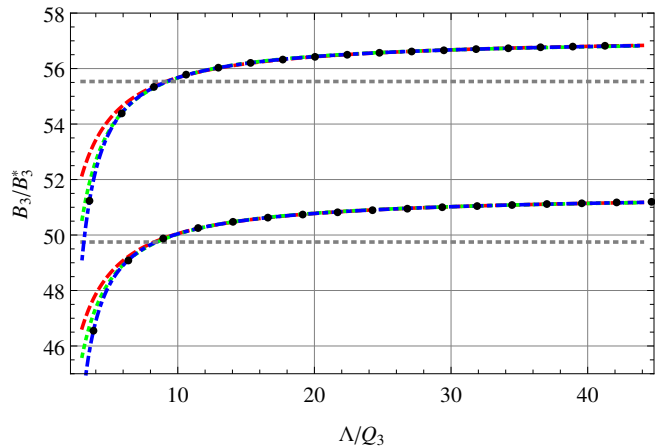


FIG. 3. (Color online) The ratio of ground-to-excited-state binding energies of the  ${}^4\text{He}$  trimer,  $B_3/B_3^*$ , for various cutoff values  $\Lambda$ , in units of the asymptotic ground-state binding momentum  $Q_3$ . The upper and lower (black) circles correspond to the LO EFT calculation based on, respectively, LM2M2 and PCKLJS potentials. The horizontal (gray) dashed lines indicate the values calculated directly from the corresponding potential [37]. Also plotted are fits to powers of  $Q_3/\Lambda$  in Eq. (22) cut after the first (red dashed lines), second (green dotted lines) and third (blue dot-dashed lines) terms.

$B_3(\infty)/B_3^* \simeq 51.50(3)$ , corresponding to  $Q_3 \simeq 0.046 a_0^{-1}$ . For the asymptotic value we took the mean of the various fits, and the error given above reflects only their spread. A naive estimate of the relative truncation error is  $Q_3 r_2/2 \sim 0.3$ , while cutoff variation gives about 0.1, because the magnitude of the dominant coefficient  $\alpha_3$  is  $\sim 1/3$ . For comparison, the ratio calculated directly from the potentials is 55.53 and 49.75 for LM2M2 and PCKLJS, respectively [37]. This agreement at the 5% level is somewhat accidental, since we have noticed that fitting the two-body LEC to the scattering length  $a_2$  instead of the binding energy  $B_2$  results in an agreement at the 20% level instead. In Table IV, we list  $B_3(\infty)/B_3^*$  for these potentials depending on the input used, either  $B_2$  or  $a_2$ . Presumably, carrying out the EFT expansion around the dimer pole in the complex momentum plane instead of the origin is better because one starts closer to the positions of the poles representing more-particle bound states [47, 48]. Therefore, below we continue to use  $B_2$  as input. Since the two fitting procedures differ by NLO terms, we assign a relative error of about 0.2 to our LO result, which makes the extrapolation error completely negligible.

As for two bosons, we can look at predictions for scattering as well. To avoid dealing with continuum wave functions, we put our system in an isotropic harmonic trap of frequency  $\omega$  and calculate the two-body ( $E_2$ ) and three-body ( $E_3$ ) energies for various trapping frequencies. As the trap is weakened, that is,  $\omega$  becomes small, the lowest two- and three-body states approach the free dimer and the free trimers, while higher states

TABLE IV. Asymptotic values of the trimer ground-state energy in units of the excited-trimer binding energy, depending on the two-atom input: dimer binding energy or scattering length. The upper (lower) results correspond to the LM2M2 (PCKLJS)-based EFT. The error is only that which comes from the fitting procedure. Also, for comparison we list the values obtained [37] directly from the corresponding potential.

input	$B_3(\infty)/B_3^*$
$B_2 = 1.3094$ mK	57.15(4)
$a_2 = 100.23$ Å	65.30(3)
direct [37]	55.53
$B_2 = 1.6154$ mK	51.50(3)
$a_2 = 90.42$ Å	59.81(2)
direct [37]	49.75

form the respective scattering continua. For the three-body system, the energies above the dimer energy can be used to extract atom-dimer scattering parameters, as long as the harmonic-oscillator length  $a_{ho} = 1/\sqrt{2\mu\omega}$ , where  $\mu \simeq 2m/3$  is the atom-dimer reduced mass, is larger than the dimer size  $\sim a_2$ . In this case, we can treat the dimer as a point-like particle, and the solution for two-body scattering inside a trap [49, 50] can be used to extract the free-space scattering parameters. For sufficiently small  $E_3$ ,

$$\sqrt{2}l \frac{\Gamma[(3-\eta)/4]}{\Gamma[(1-\eta)/4]} \simeq \frac{a_2}{a_3} \left( 1 - \frac{a_3 r_3}{4a_2^2} \eta l^2 \right), \quad (23)$$

where  $\eta = 2(E_3 - E_2)/\omega$ ,  $l = a_2/a_{ho}$ , and  $a_3$  and  $r_3$  are the atom-dimer scattering length and effective range, respectively.

Results for the left-hand side of Eq. (23) at a cutoff  $\Lambda/Q_3^* = 27.5$  are given as a function of  $\eta l^2$  in Fig. 4. Fitting them with the right-hand side of Eq. (23) allows us to extract  $a_3$  and  $r_3$  at that cutoff. The resulting atom-dimer scattering length  $a_3$  is shown in Fig. 5 for various cutoff values. We fit the cutoff dependence with

$$\frac{a_3(\Lambda)}{a_2} = \frac{a_3(\infty)}{a_2} \left[ 1 + \tilde{\alpha}_3 \frac{Q_3^*}{\Lambda} + \tilde{\beta}_3 \left( \frac{Q_3^*}{\Lambda} \right)^2 + \tilde{\gamma}_3 \left( \frac{Q_3^*}{\Lambda} \right)^3 + \dots \right]. \quad (24)$$

The resulting parameters are summarized in Table V and the corresponding curves plotted in Fig. 5. Again, convergence to the zero-range limit is good. The asymptotic value is  $a_3(\infty) = 1.153(1)a_2$  ( $a_3(\infty) = 1.322(1)a_2$ ) for the EFT based on the LM2M2 (PCKLJS) values. An estimate of the relative truncation error is  $Q_3^* r_2/2 \sim 0.1$ , since our most important source of systematic error here is the determination of the three-body force parameter.

The atom-dimer scattering length was first shown by Efimov [51] to have a log-periodic structure in  $a_2 \Lambda_*$ , a result which was reproduced in EFT [6, 7]. Several authors

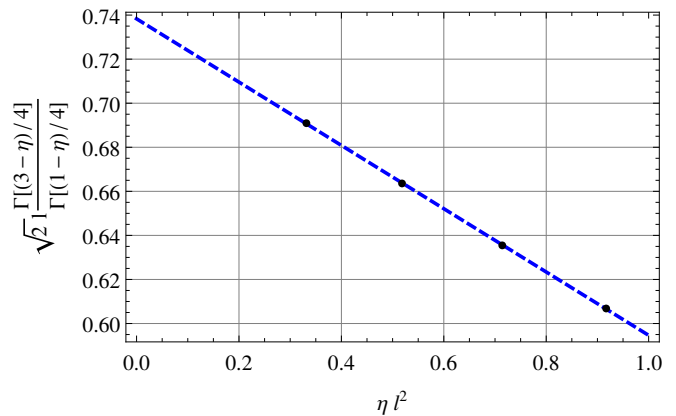


FIG. 4. (Color online) The left-hand side of Eq. (23) as a function of  $\eta$ , the difference between three- and two-body energies in units of half the harmonic oscillator frequency, multiplied by  $l^2 = (a_2/a_{ho})^2$ , at a cutoff  $\Lambda/Q_3^* = 27.5$ . Also plotted is the fit with the right-hand side of Eq. (23).

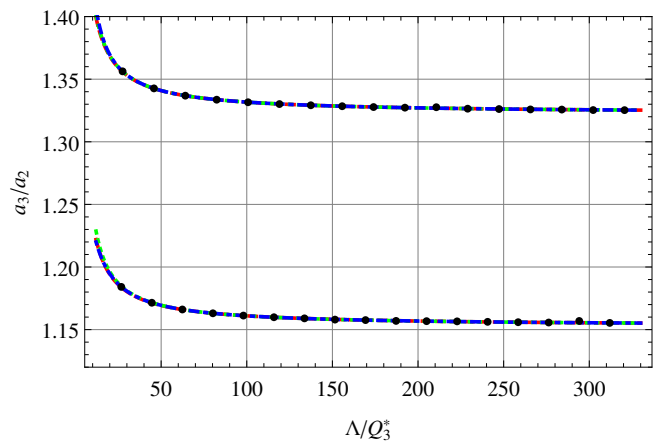


FIG. 5. (Color online) The ratio of the atom-dimer scattering length  $a_3$  to the two-atom scattering length  $a_2$  for various cutoff values  $\Lambda$  in units of  $Q_3^*$ . The upper and lower (black) circles correspond to the LO EFT calculation based on, respectively, PCKLJS and LM2M2 potentials. Also plotted are fits to powers of  $Q_3^*/\Lambda$  in Eq. (24), cut after the first (red dashed lines), second (green dotted lines) and third (blue dot-dashed lines) terms.

calculated this quantity using various  $^4\text{He}$ - $^4\text{He}$  potentials. In Table VI we summarize the available results for the LM2M2 potential, and compare them with our asymptotic value. The results from Ref. [32] are in (marginal) agreement with ours, considering our truncation error. We agree very well with the very precise results of Refs. [33–35, 38], and with the LO EFT result of Ref. [39]. Higher ERE parameters can be obtained similarly.

At NLO, no new three-body force is necessary for renormalization [7], and corrections linear in  $r_2$  can be predicted [10]. At N<sup>2</sup>LO, a two-derivative three-body force appears [11] and a second three-body input is



TABLE V. Dimensionless parameters of the fit (24) to the atom-dimer scattering length. The upper (lower) results correspond to the LM2M2- (PCKLJS-) based EFT.

$a_3(\infty)/a_2$	$\tilde{\alpha}_3$	$\tilde{\beta}_3$	$\tilde{\gamma}_3$
1.153	0.72	—	—
1.153	0.70	1.03	—
1.153	0.71	1.11	-14.2
1.322	0.69	—	—
1.322	0.69	0.21	—
1.322	0.70	-0.54	15.3

TABLE VI. The  $^4\text{He}$  atom-dimer scattering length in units of the atom-atom scattering length, as calculated with the LM2M2 potential, and with LO EFT in Ref. [39] and in this work. The cited error for our result reflects only uncertainties in the extrapolation procedure; for an extensive discussion of systematic errors, see Sec. IV B.

Ref.	[32]	[33]	[34, 35, 38]	[39]	this work
$a_3/a_2$	1.26	1.152(5)	1.151(2)	1.128	1.153(1)

needed. Taking it to be  $a_3$ , Ref. [11] presents results for the atom-dimer phase shifts and the trimer ground state. Comparing with the LO results from Refs. [6, 7], reasonable convergence with order is found.

### C. Four, five and six bosons

We have seen that a three-body counterterm is needed to stabilize the three-body system. Are more terms needed to stabilize heavier systems?

The answer for  $N = 4$  is believed to be known: no four-body counterterm is needed at LO. This is a consequence of the apparent convergence with the cutoff of the calculated tetramer energy, at least for one regulator function and a certain cutoff range [13, 14]. It is manifested in a correlation between the tetramer and trimer binding energies for fixed dimer energies but different values of  $\Lambda_*$ . In nuclear physics, the equivalent correlation between the  $^4\text{He}$  and  $^3\text{H}$  binding energies calculated with different nuclear potentials is known as the Tjon line [15].

Pushing the number of particles up, do we need to add other counterterms? In the nuclear case, where there are four-state fermions (protons and neutrons with spin up and down), such a counterterm would involve at least two derivatives because Pauli exclusion forbids more than four nucleons to come together. Indeed, the binding energy of  $^6\text{Li}$  was calculated within a similar EFT and seems to be converged without additional counterterms [22]. However, is the same true also for bosons, where

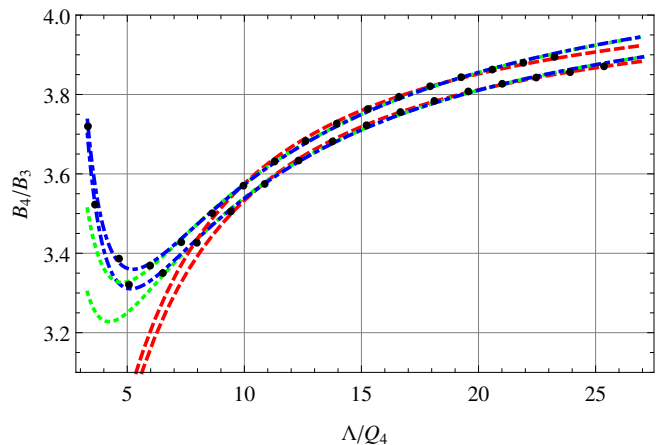


FIG. 6. (Color online) The ratio of the ground-state energies of the  $^4\text{He}$  tetramer and trimer,  $B_4/B_3$ , for various cutoff values  $\Lambda$ , in units of the asymptotic tetramer binding momentum  $Q_4$ . The upper and lower (black) circles correspond to the LO EFT calculation based on, respectively, LM2M2 and PCKLJS potentials. Also plotted are fits to powers of  $Q_4/\Lambda$  in Eq. (25) cut after the first (red dashed line), second (green dotted) and third (blue dot-dashed) terms.

no-derivative contact counterterms exist?

Here we calculate the tetramer, pentamer, and hexamer ground-state energies at LO. We show that these energies converge as the cutoff is increased, dispensing with the need for higher-body interactions at this order. We also construct generalized Tjon lines.

The ratio of the tetramer and trimer ground-state energies is plotted in Fig. 6 for various cutoffs. The corresponding plots for the pentamer and hexamer ground-state energies are presented in Figs. 7 and 8, respectively. Convergence is evident. To strengthen the argument, we again fit the numerical results with expressions of the type

$$\frac{B_N(\Lambda)}{B_3(\Lambda)} = \frac{B_N(\infty)}{B_3(\infty)} \left[ 1 + \alpha_N \frac{Q_N}{\Lambda} + \beta_N \left( \frac{Q_N}{\Lambda} \right)^2 + \gamma_N \left( \frac{Q_N}{\Lambda} \right)^3 + \dots \right], \quad (25)$$

where  $Q_N$  is calculated from  $B_N(\infty)$  via Eq. (2). The corresponding curves truncated at successive terms are also shown in Figs. 6, 7, and 8.

The fitting parameters for  $N = 4$  are shown in Table VII. The values are somewhat larger than for the ground-state trimer in Table III, reflecting slower convergence. But they still can be considered natural, suggesting that the tetramer is likely within the EFT despite being considerably more bound than the trimer. Although we cannot fully exclude a mild  $\ln \Lambda$  divergence, adding such a term to Eq. (25) requires a much smaller coefficient. Thus we confirm, with a different regulator than in Ref. [13, 14], that no four-body force is needed at LO. Our

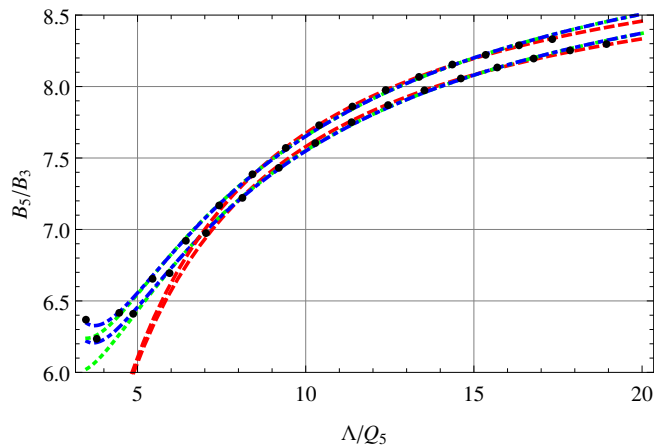


FIG. 7. (Color online) The ratio of the ground-state energies of the  ${}^4\text{He}$  pentamer and trimer,  $B_5/B_3$ , for various cutoff values  $\Lambda$ , in units of the asymptotic pentamer binding momentum  $Q_5$ . The upper and lower (black) circles correspond to the LO EFT calculation based on, respectively, LM2M2 and PCKLJS potentials. Also plotted are fits to powers of  $Q_5/\Lambda$  in Eq. (25) cut after the first (red dashed lines), second (green dotted lines) and third (blue dot-dashed lines) terms.

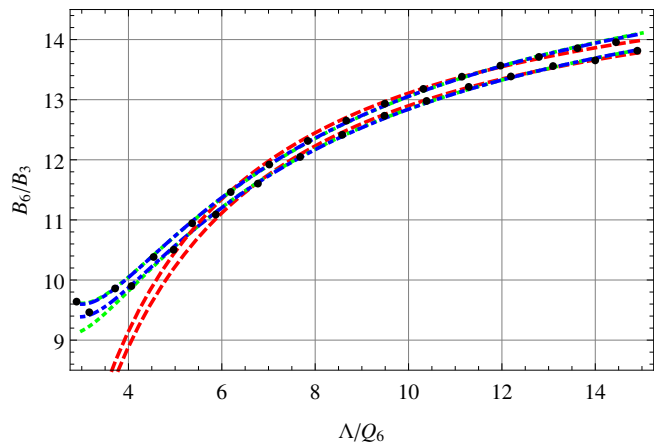


FIG. 8. (Color online) The ratio of the ground-state energies of the  ${}^4\text{He}$  hexamer and trimer,  $B_6/B_3$ , for various cutoff values  $\Lambda$ , in units of the asymptotic hexamer binding momentum  $Q_6$ . The upper and lower (black) circles correspond to the LO EFT calculation based on, respectively, LM2M2 and PCKLJS potentials. Also plotted are fits to powers of  $Q_6/\Lambda$  in Eq. (25) cut after the first (red dashed lines), second (green dotted lines) and third (blue dot-dashed lines) terms.

results are qualitatively similar for  $N = 5, 6$ . The fitting parameters  $\alpha_{5,6}$ ,  $\beta_{5,6}$ , and  $\gamma_{5,6}$  for the pentamer and the hexamer binding energies are, again, of natural size, while an  $\ln \Lambda$  term is much smaller. The good convergence of the pentamer and hexamer ground-state energies for our regulator is evidence that no five- and six-body forces are needed at LO, either.

Our converged values for the tetramer-to-trimer ratio

TABLE VII. Dimensionless parameters of the fit (25) to the tetramer-to-trimer binding-energy ratio. The upper (lower) results correspond to the LM2M2 (PCKLJS)-based EFT.

$B_4(\infty)/B_3(\infty)$	$\alpha_4$	$\beta_4$	$\gamma_4$
4.128	-1.34	—	—
4.240	-2.06	4.93	—
4.238	-2.02	4.06	4.30
4.090	-1.36	—	—
4.165	-1.90	4.02	—
4.157	-1.80	2.32	7.99

TABLE VIII. The  $N$ -body  ${}^4\text{He}$  binding energies, in units of the trimer binding energy, for  $N = 4, 5, 6$ . Our results are compared to those obtained with the PCKLJS [37], LM2M2 [32] and TTY [31] potentials, as well as a soft-core potential [19]. The cited errors for our results reflect only uncertainties in the extrapolation procedure; for an extensive discussion of systematic errors, see Sec. IV C.

Ref.	[37]	[32]	[31]	[19]	this work
$B_4/B_3$	4.35	4.44(1)	4.49(2)	4.500	4.20(6)
$B_5/B_3$	—	10.33(1)	10.519(8)	10.495	9.5(2)
$B_6/B_3$	—	18.41(2)	18.50(2)	18.504	16.3(5)

of ground-state energies are  $B_4(\infty)/B_3(\infty) \simeq 4.20(6)$  and  $4.14(4)$  for LM2M2 and PCKLJS potentials, respectively. This is to be compared with the corresponding values predicted directly from these potentials, respectively  $4.42$  and  $4.35$  [37]. Similarly, we find that our converged values for the pentamer-to-trimer ratio of ground-state energies are  $B_5(\infty)/B_3(\infty) \simeq 9.5(2)$  and  $9.3(2)$  for LM2M2 and PCKLJS, respectively. For the hexamer-to-trimer ratio, we find  $B_6(\infty)/B_3(\infty) \simeq 16.3(5)$  for LM2M2 and  $16.0(4)$  for PCKLJS. We are not aware of five- nor six-body calculations using the PCKLJS potential. The values predicted directly from the LM2M2 potential are  $10.33(1)$  for pentamer and  $18.41(2)$  for hexamer [32]. In Table VIII we summarize the binding energies ratios for  $N \geq 4$  systems, as well as available results calculated directly from  ${}^4\text{He}$ - ${}^4\text{He}$  potentials.

The errors reported above are only fitting errors. Our naive systematic error is much larger, ranging from 55% for  $N = 4$  to 90% for  $N = 6$ , if we use  $Q_N r_2/2 \sim (r_2/2a_2)\sqrt{2B_N/NB_2}$  for an estimate. Cutoff variation gives similar estimates, since the fitting parameters are  $\mathcal{O}(1)$ . Yet, compared with values obtained directly from the LM2M2 potential [32], our central values for energy ratios are off by only about 5% for  $N = 4$  and 15% for  $N = 6$ . The soft-core potential of Refs. [19, 21] resembles our LO supplemented by some higher-order corrections, so we might expect that NLO will supply most of the dif-

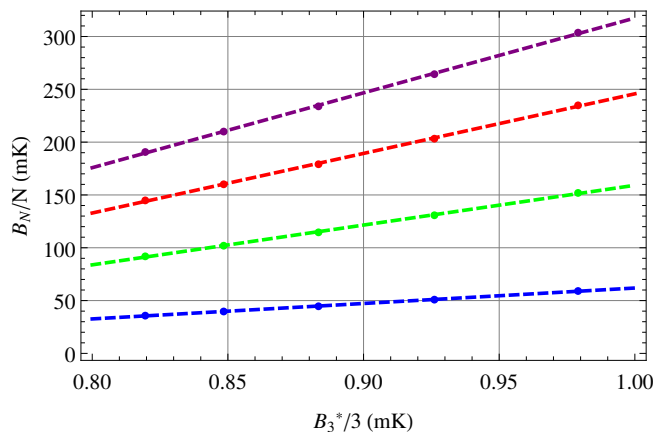


FIG. 9. (Color online) Generalized Tjon lines: binding energies per particle,  $B_N/N$ , in mK for the  $N = 3$  (blue, bottom), 4 (green, second from bottom), 5 (red, third from bottom) and 6 (purple, top) ground states for various values of the trimer excited-state energy per particle,  $B_3^*/3$ , in mK, at fixed dimer binding energy  $B_2$ . Here we used  $B_2 = 1.6154$  mK and  $\Lambda \simeq 1.22 \text{ \AA}^{-1}$ . Linear fits are also shown.

ference between our results and those of Ref. [32]. This suggests that  $Q_N r_2/2$ , with  $Q_N$  defined by Eq. (2), is an overestimate of the systematic error. Note that the spread among potential models, which differ in the details of short-range physics, is only about 2%. It seems that, despite the increasing binding, most of the dynamics of these atomic droplets takes place at distances larger than  $r_{\text{vdW}}$ , with  $1/Q_N$  an underestimate of the relevant distance.

The absence of higher-body forces at LO means that, for fixed two-body input, the LO energies of not only the ground tetramer, but also of the ground pentamer and hexamer are determined by the three-body parameter. Since we use the excited trimer energy as input, the same is true, as we have seen in Sec. IV B, for the ground trimer. As a consequence, these energies are all correlated. Next we vary  $Q_3^*$  at fixed  $B_2$ , therefore changing  $B_3^*$ , and calculate  $B_3$ ,  $B_4$ ,  $B_5$ , and  $B_6$ . The generalized Tjon lines are plotted in Fig. 9, where the correlation between the ground-state binding energies  $B_N/N$  and  $B_3^*/3$  is evident. The results presented in Fig. 9 were obtained for a dimer binding energy  $B_2 = 1.6154$  mK and a cutoff  $\Lambda \simeq 1.22 \text{ \AA}^{-1}$ . Qualitatively similar results are obtained for higher cutoffs. In the region we focus on, the generalized Tjon lines are approximately straight with a derivative that increases monotonically with  $N$ . The corresponding linear fits are also shown in Fig. 9.

Changing  $B_2$ , line positions change, but not, of course, the fact that a correlation exists among the various energies. On dimensional grounds we can write

$$\frac{B_N}{N} = c_N(B_2/B_3^*) \frac{B_3^*}{3}, \quad (26)$$

where the  $c_N(B_3^*/B_2)$  are universal, dimensionless functions of the only dimensionless ratio at LO,  $B_3^*/B_2$ .

(At finite cutoff,  $c_N$  depends also on  $Q_3^*/\Lambda$ .) Results from phenomenological two-body potentials with similar dimer binding energies should fall on or close to these lines. Because the scattering length of the  $^4\text{He}$  dimer is so large, this system is relatively close to the unitarity limit in the sense that the first Efimov excited state exists. The generalized Tjon lines at unitarity, while not exactly the same as those in Fig. 9, are not very different. Expanding in a series in  $B_2/B_3^*$ ,

$$\frac{B_N}{N} = c_N(0) \frac{B_3^*}{3} + \dots, \quad (27)$$

in terms of the universal set of numbers  $c_N(0)$ . Eliminating  $B_3^*$  in favor of  $B_3$ ,

$$\frac{B_N}{B_3} \approx \frac{N c_N(0)}{3 c_3(0)} \approx (N-2)^2, \quad (28)$$

where the last approximation summarizes our converged values in Table VIII. Since  $B_2/B_3 \approx 10^{-2}$ , Eq. (28) applies to  $N = 2$  as well.

Near unitarity, then, the physics of few-boson clusters is essentially determined by the single parameter,  $\Lambda_*$ , that fixes  $B_3$ . Moreover, the  $N$  dependence is particularly simple:  $B_N/B_3$  seems to grow as  $N^2$  as noticed in Ref. [52]. In fact, our  $N \leq 6$  results, even though not quite at unitarity, are well described by the empirical relation [53]

$$\frac{B_N}{B_3} \approx \left[ (N-3) \sqrt{\frac{B_4}{B_3}} + 4 - N \right]^2, \quad (29)$$

which reduces to  $(N-2)^2$  for  $B_4/B_3 \approx 4$ . Our results in Table VIII differ by less than 15% from the  $N \leq 6$  ground-state ratios at unitarity obtained with a particular potential [18, 20]. Note that the latter ratios are more consistent with

$$(N-2)^2 \rightarrow \frac{N(N-1)(N-2)}{6},$$

in Eq. (28) and we cannot exclude such form. However, the  $7 \leq N \leq 10$  values for the ratio  $B_N/B_3$  in Ref. [18] are in much better agreement with  $(N-2)^2$ , and for  $N \geq 11$  energies grow even slower. Ground-state ratios calculated from other potentials [23, 54] show different trends as  $N$  increases, but tend to agree with Eq. (29). In EFT, saturation arises from a balance between two- and three-body forces, and the latter cannot be separated from the high-momentum components of the former in a cutoff-independent way. In this context there is no obvious argument to justify a dependence on  $N$  of one form or another. An EFT calculation along the lines of this paper but for a wider range of  $N$  values would be highly desirable.

## V. CONCLUSION

Summing up, we constructed an effective field theory for the few-boson system. We have solved the leading-

order Schrödinger equation for up to six particles using a correlated Gaussian basis and the stochastic variational method. We have shown that various observables converge as the arbitrary ultraviolet cutoff increases. The extrapolation to the infinite-cutoff limit corresponds to a zero-range interaction. It is therefore safe to assume that the dominant features of bosonic systems, when within the domain of validity of EFT, are described by two parameters: the coefficients of the contact two- and three-body forces, which encode the two-body scattering length  $a_2$  (or the dimer binding energy  $B_2$ ) and a three-body parameter  $\Lambda_*$  (or a trimer binding energy). Generalized Tjon lines were introduced, showing the correlation among the ground-state energies of three, four, five and six particles when  $\Lambda_*$  is varied at fixed  $a_2$ .

For concreteness, we have presented results for  ${}^4\text{He}$  systems. As input, we could have used the experimental values for the binding energies of the dimer,  $B_2$ , and of the excited trimer,  $B_3^*$ . In order to gauge the convergence of the EFT, we opted instead to use values from two modern  ${}^4\text{He}$ - ${}^4\text{He}$  potentials, LM2M2 and PCKLJS. These are representative of the experimental data, and therefore our numbers for other observables can be seen as EFT predictions. At the same time, they allow us to compare our results with few-body energies obtained directly from these potentials. The latter energies contain information not only about  $B_2$  and  $B_3^*$ , but also about a host of other  ${}^4\text{He}$  properties. The point of an EFT is that this extra information is only relevant in a marginal way, as we proceed to higher orders. This is, of course, true only for observables for which the EFT expansion converges.

Our results for  ${}^4\text{He}$  systems are in surprisingly good agreement with the literature. They reproduce the LO results of Refs. [11] and [13] for  $N = 3$  and 4, respectively, and extend LO contact EFT to  $N = 5, 6$ . The ground-state energies we calculate agree with direct results from the same potential at a level that ranges from about 5% at  $N = 3$  to 15% at  $N = 6$ . In contrast, a naive estimate based on the range of the potential and Eq. (2) as an estimate of the particle binding momentum gives much larger errors. If not accidental, this agreement would imply that the range of applicability of the EFT is much wider than expected. Such optimism has become part of EFT folklore since a good description was obtained in nuclear physics for the triton [55] and, especially, the relatively tight *alpha* particle [56], even though  ${}^9\text{Li}$  [22] did not come out particularly well despite having a similar binding energy per particle. Here we have added circumstantial evidence that the EFT expansion works well beyond  $N = 3$   ${}^4\text{He}$  atoms. Systems within the range of applicability of contact EFT share the same dynamical origin as the three-body states that are usually labeled “Efimov states.”

Note that the PCKLJS potential gives about 30% more binding energy for the dimer compared to LM2M2. Heavier systems are also more bound for PCKLJS, but the excited and ground-state trimers are more bound by just 15% and 5%, respectively. Our  $N = 4, 5, 6$  ground-state energies for these potentials also differ by 5% or less. It seems that, once  $B_3$  is obtained correctly,  $B_{4,5,6}$  follow. This pattern is consistent with potentials having similar values of  $\Lambda_*$ , which determine the larger  $B_{3,4,5,6}$ , but somewhat different values of the large  $a_2$ , which affect primarily the smaller  $B_2$  and  $B_3^*$ . Perhaps the LO error in  $B_3$ , which we estimated at 20%, is also a reasonable estimate of the error in  $B_{4,5,6}$ .

While we have presented results for  ${}^4\text{He}$  systems, qualitatively similar results are obtained for other systems with large scattering lengths, including the unitarity limit  $1/a_2 = 0$ . The EFT captures Efimov physics at LO, where  $\Lambda_*$  determines the position of the geometric ladder of three-body bound states. In systems with more particles,  $\Lambda_*$  also sets the scale for the binding energies. For  $N \leq 6$ , energies have the simple approximate scaling in Eq. (28) or a similar form. That  $Q_3 r_2/2$  might be a more realistic error estimate than  $Q_N r_2/2$  is consistent with the observation in Ref. [23] that the average interparticle distance at unitarity is more or less constant with  $N$ , and of  $\mathcal{O}(1/Q_3)$ .

Thus an EFT expanded around the zero-range limit captures the essence of universal bosonic systems. Corrections to the zero-range limit, such as the two-body effective range  $r_2$ , appear at next-to-leading order. Stronger arguments than presented here about the convergence of the EFT expansion require higher-order calculations. We plan to extend our calculation to NLO in a future publication.

## ACKNOWLEDGMENTS

We acknowledge useful discussions with N. Barnea, T. Frederico, and H.-W. Hammer. B.B. and U.v.K. thank the Institute for Nuclear Theory at the University of Washington for its hospitality during the Program INT-16-1 “Nuclear Physics from Lattice QCD,” when part of this work was carried out. This material is based upon work supported in part by a Chateaubriand Fellowship of the French Embassy in Israel (B.B.), by the Pazi Fund (M.E.), by France’s Centre National de la Recherche Scientifique under a grant of IN2P3’s Comité de Financement des Projets de Physique Théorique (U.v.K.), and by the U.S. Department of Energy, Office of Science, Office of Nuclear Physics, under Award no. DE-FG02-04ER41338 (U.v.K.).

---

[1] V. Efimov, “Energy levels arising from the resonant two-body forces in a three-body system”, Phys. Lett. B **33**, 563

(1970).

- [2] E. Braaten and H.-W. Hammer, “Universality in few-body systems with large scattering length”, *Phys. Rep.* **428**, 258 (2006).
- [3] F. Luo, C.F. Giese and W.R. Gentry, “Direct measurement of the size of the helium dimer”, *J. Chem. Phys.* **104**, 1151 (1996).
- [4] C. Chin, R. Grimm, P. Julienne, and E. Tiesinga, “Feshbach resonances in ultracold gases”, *Rev. Mod. Phys.* **82**, 1225 (2010).
- [5] U. van Kolck, “Effective field theory of short-range forces”, *Nucl. Phys. A* **645**, 273 (1999).
- [6] P.F. Bedaque, H.-W. Hammer, and U. van Kolck, “Renormalization of the three-body system with short-range interactions”, *Phys. Rev. Lett.* **82**, 463 (1999).
- [7] P.F. Bedaque, H.-W. Hammer, and U. van Kolck, “The three boson system with short-range interactions”, *Nucl. Phys. A* **646**, 444 (1999).
- [8] R.F. Mohr, R.J. Furnstahl, H.-W. Hammer, R.J. Perry and K.G. Wilson, “Precise numerical results for limit cycles in the quantum three-body problem”, *Annals Phys.* **321**, 225 (2006).
- [9] A.C. Phillips, “Consistency of the low-energy three-nucleon observables and the separable interaction model”, *Nucl. Phys. A* **107**, 209 (1968).
- [10] C. Ji, D.R. Phillips and L. Platter, “The three-boson system at next-to-leading order in an effective field theory for systems with a large scattering length”, *Annals Phys.* **327**, 1803 (2012).
- [11] C. Ji and D.R. Phillips, “Effective field theory analysis of three-boson systems at next-to-next-to-leading order”, *Few-Body Syst.* **54**, 2317 (2013).
- [12] H.W. Griefhammer, “Naive dimensional analysis for three-body forces without pions”, *Nucl. Phys. A* **760**, 110 (2005).
- [13] L. Platter, H.-W. Hammer and U.-G. Meißner, “The four-boson system with short-range interactions”, *Phys. Rev. A* **70**, 052101 (2004).
- [14] H.-W. Hammer and L. Platter, “Universal properties of the four-body system with large scattering length”, *Eur. Phys. J. A* **32**, 113 (2007).
- [15] J.A. Tjon, “Bound states of  $^4\text{He}$  with local interactions”, *Phys. Lett. B* **56**, 217 (1975).
- [16] M.R. Hadizadeh, M.T. Yamashita, L. Tomio, A. Delfino and T. Frederico, “Universality and scaling limit of weakly-bound tetramers”, *Phys. Rev. Lett.* **107**, 135304 (2011).
- [17] T. Frederico, A. Delfino, M.R. Hadizadeh, L. Tomio and M.T. Yamashita, “Universality in four-boson systems”, *Few-Body Syst.* **54**, 559 (2013).
- [18] J. von Stecher, “Weakly bound cluster states of Efimov character”, *J. Phys. B* **43**, 101002 (2010).
- [19] M. Gattobigio, A. Kievsky and M. Viviani, “Spectra of helium clusters with up to six atoms using soft-core potentials”, *Phys. Rev. A* **84**, 052503 (2011).
- [20] J. von Stecher, “Five- and six-body resonances tied to an Efimov trimer”, *Phys. Rev. Lett.* **107**, 200402 (2011).
- [21] M. Gattobigio, A. Kievsky and M. Viviani, “Energy spectra of small bosonic clusters having a large two-body scattering length”, *Phys. Rev. A* **86**, 042513 (2012).
- [22] I. Stetcu, B.R. Barrett and U. van Kolck, “No-core shell model in an effective-field-theory framework”, *Phys. Lett. B* **653**, 358 (2007).
- [23] Y. Yan and D. Blume, “Energy and structural properties of  $N$ -boson clusters attached to three-body Efimov states: Two-body zero-range interactions and the role of the three-body regulator”, *Phys. Rev. A* **92**, 033626 (2015).
- [24] Y. Suzuki and K. Varga, “Stochastic Variational Approach to Quantum-Mechanical Few-Body Problems”, Springer (1998).
- [25] M. Kunitski et al., “Observation of the Efimov state of the helium trimer”, *Science* **348**, 551 (2015).
- [26] S. Nakaichi, Y. Akaishi, H. Tanaka and T.K. Lim, “Application of ATMS to the  $^4\text{He}$  trimer and tetramer”, *Phys. Lett. A* **68**, 36 (1978).
- [27] S. Nakaichi, T.K. Lim, Y. Akaishi and H. Tanaka, “Few-atom  $^3\text{He}$ - $^4\text{He}$  mixed molecules”, *J. Chem. Phys.* **71**, 4430 (1979).
- [28] T.K. Lim, S. Nakaichi, Y. Akaishi and H. Tanaka, “Near-threshold behavior of the ground-state binding energies of the few-atom systems of  $^4\text{He}$  and other bosons in two and three dimensions”, *Phys. Rev. A* **22**, 28 (1980).
- [29] R.A. Aziz and M.J. Slaman, “An examination of *ab initio* results for the helium potential energy curve”, *J. Chem. Phys.* **94**, 8047 (1991).
- [30] A.R. Janzen and R.A. Aziz, “Modern He-He potentials: Another look at binding energy, effective range theory, retardation, and Efimov states”, *J. Chem. Phys.* **103**, 9626 (1995).
- [31] M. Lewerenz, “Structure and energetics of small helium clusters: Quantum simulations using a recent perturbational pair potential”, *J. Chem. Phys.* **106**, 4596 (1997).
- [32] D. Blume and C.H. Greene, “Monte Carlo hyperspherical description of helium cluster excited states”, *J. Chem. Phys.* **112**, 8053 (2000).
- [33] E.A. Kolganova, A.K. Motovilov, and W. Sandhas, “Scattering length of the helium atom helium dimer collision”, *Phys. Rev. A* **70**, 052711 (2004).
- [34] V. Roudnev, “Ultra-low energy elastic scattering in a system of three He atoms”, *Chem. Phys. Lett.* **367**, 95 (2003).
- [35] R. Lazauskas and J. Carbonell, “Description of  $^4\text{He}$  tetramer bound and scattering states”, *Phys. Rev. A* **73**, 062717 (2006).
- [36] M. Przybytek, W. Cencek, J. Komasa, G. Lach, B. Jeziorski and K. Szalewicz, “Relativistic and quantum electrodynamics effects in the helium pair potential”, *Phys. Rev. Lett.* **104**, 183003 (2010).
- [37] E. Hiyama and M. Kamimura, “Variational calculation of  $^4\text{He}$  tetramer ground and excited states using a realistic pair potential”, *Phys. Rev. A* **85**, 022502 (2012).
- [38] A. Deltuva, “Momentum-space calculation of  $^4\text{He}$  triatomic system with realistic potential”, *Few-Body Syst.* **56**, 897 (2015).
- [39] E. Braaten and H.-W. Hammer, “Universality in the three-body problem for  $^4\text{He}$  atoms”, *Phys. Rev. A* **67**, 042706 (2003).
- [40] L.H. Thomas, “The interaction between a neutron and a proton and the structure of  $H^3$ ”, *Phys. Rev.* **47**, 903 (1935).
- [41] P.F. Bedaque and U. van Kolck, “Effective field theory for few-nucleon systems”, *Ann. Rev. Nucl. Part. Sci.* **52**, 339 (2002).
- [42] Z.-C. Yan, J.F. Babb, A. Dalgarno, and G.W.F. Drake, “Variational calculations of dispersion coefficients for interactions among H, He, and Li atoms”, *Phys. Rev. A* **54**, 2824 (1996).

- [43] J.-Y. Zhang, Z.-C. Yan, D. Vranceanu, J.F. Babb, and H.R. Sadeghpour, “*Long-range interactions for  $He(nS)He(n'S)$  and  $He(nS)He(n'P)$* ”, Phys. Rev. A **74**, 014704 (2006).
- [44] W. Cencek, M. Przybytek, J. Komasa, J.B. Mehl, B. Jezierski, and K. Szalewicz, “*Effects of adiabatic, relativistic, and quantum electrodynamics interactions on the pair potential and thermophysical properties of helium*”, J. Chem. Phys. **136**, 224303 (2012).
- [45] R.E. Grisenti, W. Schollkopf, J.P. Toennies, G.C. Hegerfeldt, T. Kohler and M. Stoll, “*Determination of the bond length and binding energy of the Helium dimer by diffraction from a transmission grating*”, Phys. Rev. Lett. **85**, 2284 (2000).
- [46] S. Zeller et al., “*Imaging the  $He_2$  quantum halo state using a free electron laser*”, arXiv:1601.03247 [physics.atom-ph] (2016).
- [47] D.R. Phillips, G. Rupak and M.J. Savage, “*Improving the convergence of NN effective field theory*”, Phys. Lett. B **473**, 209 (2000).
- [48] H.W. Griesshammer, “*Improved convergence in the three-nucleon system at very low energies*”, Nucl. Phys. A **744**, 192 (2004).
- [49] T. Busch, B.-G. Englert, K. Rzażewski and M. Wilkens, “*Two cold atoms in a harmonic trap*”, Found. Phys. **28**, 549 (1998).
- [50] I. Stetcu, J. Rotureau, B.R. Barrett, and U. van Kolck, “*An effective field theory approach to two trapped particles*”, Annals Phys. **325**, 1644 (2010).
- [51] V. Efimov, Yad. Fiz. **29**, 1058 (1979) [“*Low-energy properties of three resonantly-interacting particles*”, Sov. J. Nucl. Phys. **29**, 546 (1979)].
- [52] A.N. Nicholson, “*N-body Efimov states from two-particle noise*”, Phys. Rev. Lett. **109**, 073003 (2012).
- [53] M. Gattobigio and A. Kievsky, “*Universality and scaling in the N-body sector of Efimov physics*”, Phys. Rev. A **90**, 012502 (2014).
- [54] A. Kievsky, N.K. Timofeyuk and M. Gattobigio, “*N-boson spectrum from a discrete scale invariance*”, Phys. Rev. A **90**, 032504 (2014).
- [55] P.F. Bedaque, H.-W. Hammer and U. van Kolck, “*Effective theory of the triton*”, Nucl. Phys. A **676**, 357 (2000).
- [56] L. Platter, H.-W. Hammer and U.-G. Meißner, “*On the correlation between the binding energies of the triton and the alpha-particle*”, Phys. Lett. B **607**, 254 (2005).